Fachtagung "Lasermethoden in der Strömungsmesstechnik"
7. – 9. September 2004, Universität Karlsruhe

EFFECT OF FRINGE DIVERGENCE IN FLUID ACCELERATION MEASUREMENT USING LDA

Sejong Chun[1], Holger Nobach[2], Nils Damaschke[2], Nikolay Semidetnov[2], Cam Tropea[2]

[1] Department of Mechanical Engineering, Korea Advanced Institute of Science and Technology, 305-701, Daejeon, Korea
[2] Fachgebiet Strömungslehre und Aerodynamik, Technische Universität Darmstadt, Petersenstraße 30, 64287 Darmstadt, Germany

E-mail : schun@sla.tu-darmstadt.de

1. Introduction

The laser Doppler technique is well-established as a velocity measurement technique of high precision for flow velocity. Recently, the laser Doppler technique has also been used to measure acceleration of fluid particles (Lehmann et al. 2002). Acceleration is interesting from a fluid mechanics point of view, since the Navier Stokes equations, specifically the left-hand-side, are formulated in terms of fluid acceleration. Further, there are several avenues to estimating the dissipation rate using the acceleration (Mann et al. 1999). However such measurements place additional demands on the design of the optical system; in particular fringe non-uniformity must be held below about 0.01% to avoid systematic errors. Relations expressing fringe divergence as a function of the optical parameters of the system have been given in the literature (Miles 1996, Miles and Witze 1996); however, direct use of these formulae to minimize fringe divergence lead either to very large measurement volumes or to extremely high intersection angles (Lehmann et al 2002). This dilemma can be resolved by using an off-axis receiving arrangement, in which the measurement volume is truncated by a pinhole in front of the detection plane. In the present study an optical design study is performed for optimizing laser Doppler systems for fluid acceleration measurements. This is followed by laboratory validation using a round free jet and a stagnation flow, two flows in which either fluid acceleration has been previously measured or in which the acceleration is known analytically. A 90 degree off-axis receiving angle is used with a pinhole.

2. Design Considerations for Fringe Divergence

Fringe divergence L is defined as a relative error of the fringe spacing at arbitrary positions, δx with respect to the fringe spacing at the origin, δx_o.

$$L = \left(\delta x - \delta x_o\right) / \delta x_o \tag{1}$$

There are two main dependencies of δx to be considered, longitudinal and transverse. The longitudinal dependency is given by (Miles 1996).

$$\delta x_z = \frac{\lambda}{2\sin\frac{\Theta}{2}}\left[\begin{array}{l} 1-\hat{z}\left(\cos\frac{\Theta}{2}\right)^2\left(\frac{r_o}{d}\right)\left(\frac{z_o-f}{l_R}\right) \\ +\hat{z}^2\left(\cos\frac{\Theta}{2}\right)^4\left(\frac{r_o}{d}\right)^2\frac{1}{1-\hat{z}\left(\cos\frac{\Theta}{2}\right)^2\left(\frac{r_o}{d}\right)\left(\frac{z_o-f}{l_R}\right)} \end{array}\right] \quad (2)$$

Here, λ is the wavelength of two laser beams, Θ is the full intersection angle of the beams, r_o is the beam diameter before the transmitting lens, d is the beam separation before the transmitting lens, z_o is the position of beam waist in front of the transmitting lens, f is the focal length of transmitting lens, l_R is the Rayleigh length, and $\hat{z}$ is the normalized beam axis, i.e., $-1 \le \hat{z} \le 1$. For an ideal beam alignment,

$$\delta x_{z,ideal} = \frac{\lambda}{2\sin\frac{\Theta}{2}}\left[1+\hat{z}^2\left(\cos\frac{\Theta}{2}\right)^4\left(\frac{r_o}{d}\right)^2\right]. \quad (3)$$

The transverse fringe spacing dependency is given by (Miles 1996),

$$\delta x_x = \frac{\lambda}{2\sin\frac{\Theta}{2}}\left[1-\hat{x}\left(\cos\frac{\Theta}{2}\right)^5\frac{r_o}{d}\frac{z_o-f}{l_R}\right] \quad (4)$$

where $\hat{x}$ is the normalized transverse axis, i.e., $-1 \le \hat{x} \le 1$. For an ideal beam alignment, the transverse fringe spacing becomes

$$\delta x_{x,ideal} = \frac{\lambda}{2\sin\frac{\Theta}{2}}. \quad (5)$$

Following the definition of fringe divergence in Eq. (1), the longitudinal fringe divergence L_z with an ideal beam alignment is then

$$L_z = \hat{z}^2\left(\cos\frac{\Theta}{2}\right)^4\left(\frac{r_o}{d}\right)^2 \quad (6)$$

The transverse fringe divergence L_x with the ideal beam alignment becomes

$$L_x = 0 \quad (7)$$

which means no fringe divergence in this situation.

L_z is symmetric about $\hat{z} = 0$ and the divergence in the z direction dominates over the transverse divergence, L_x. For fluid acceleration measurements, L should be less than about 0.01%. A design formula for a specified fringe divergence L_z is therefore

$$f/d \le \frac{1}{\tan\left(\cos^{-1}\left(\frac{L_z^{0.25}}{(r/d)^{0.5}}\right)\right)}. \quad (8)$$

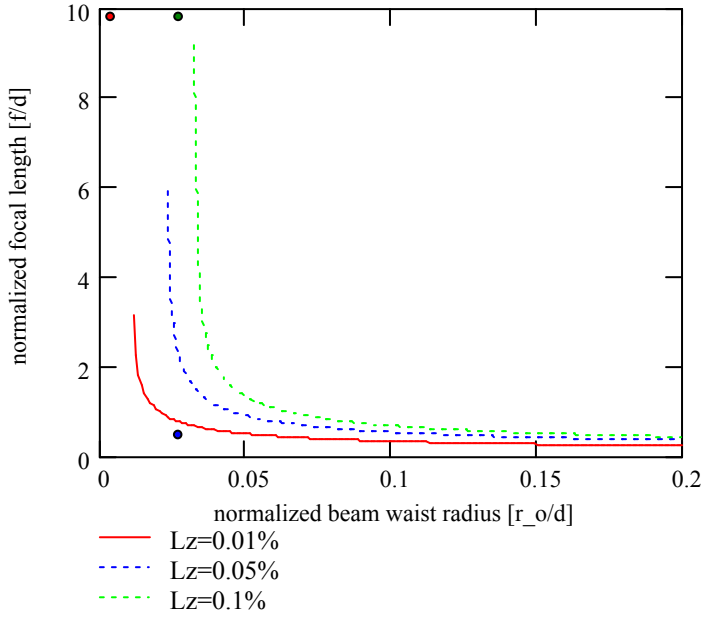

Fig. 1: Design curve for fringe divergence (dots indicate design points)

	f/d	r_o/d	f (mm)	r_o (mm)	r_w (mm)	Θ (deg)	L_x (%)	L_z (%)
Case 1	10	0.00667	300	0.2	0.245	11.4	0.4×10^{-6}	0.0044
Case 2	0.0667	0.0333	20	1	3.27×10^{-3}	112.6	0.248	0.11
Case 3	10	0.0333	300	1	0.049	11.4	0.001	0.1

Table 1: Design point for transmitting optics

Fig.1 displays design curves for different limiting fringe divergence values L_z. The areas below the solid line in Fig. 1 represent conditions under which the fringe divergence is less than 0.01%. The black dots denote design points to be used in the present study. Three design points have been selected and prescribed in more detail in Table 1. All the parameters are obtained using the above equation for L_z. Both L_z and L_x have been calculated by the fringe spacing formula without approximation for comparison purposes (Miles 1996).

$$\delta x_{x,z} = \frac{\lambda}{2\sin\frac{\Theta}{2}}\left[1+\frac{\left(\frac{x_1 z_1}{z_1^2+l_{R1}^2}-\frac{x_2 z_2}{z_2^2+l_{R2}^2}\right)}{2\tan\frac{\Theta}{2}-\left(\frac{x_1 z_1}{z_1^2+l_{R1}^2}-\frac{x_2 z_2}{z_2^2+l_{R2}^2}\right)}\right] \tag{9}$$

Here, x_i and z_i $(i=1,2)$ are local beam coordinates to describe two input laser beams. l_{Ri} $(i=1,2)$ is the Rayleigh length corresponding to each laser beam. In this case, direct derivation of fringe divergence formula would be much more complicated than Eqs. (6) and (7). The complete fringe divergence by using Eq. (9) should give good agreement with Eqs. (6) and (7).

In Table 1, Case 1 displays the situation when the size of the measurement volume is rather large and no longer a point measurement. Because the beam radius before transmitting lens is very small, the beam radius after the lens becomes larger according to (Albrecht et al. 2003).

$$r_w = \frac{\lambda f}{\pi r_o} \tag{10}$$

r_w is the beam waist radius after the transmitting lens. In Case 1, $r_w = 0.245\ mm$ is relatively large compared with the other two cases shown in Table 1. Therefore, the size of measurement volume might be treated as volumetric rather than point-wise among the three design points.

Case 2 corresponds to a highly focussed system with a large intersection angle. A large intersection angle actually violates the assumptions made in deriving the fringe spacing formulae (Miles and Witze 1996; Miles 1996).

Case 3 is a more typical optical arrangement, using an off-axis receiving optics and a pinhole. While the pinhole is normally included to remove background noise components, in this case it also truncates the measurement volume in the z direction and eliminates portions with high fringe divergence. Case 1 and 3 give very low value at L_x, which indicates the assumptions used to derive Eq. (8) are correct.

Figs. 2 – 4 illustrate the fringe divergence for each design case. Fig. 2 displays the fringe divergence in Case 1. The longitudinal fringe divergence reaches 0.005% at the edge of the measurement volume, while the transverse fringe divergence is essentially zero. Fig. 3 displays the fringe divergence in Case 2. Significant deviation from the approximate fringe divergence formulae is found, because a very large intersection angle is used. In this case, the transverse fringe divergence seems to dominate the fringe divergence. However, this results simply shows the violation of assumptions mentioned above. Fig. 4 displays the fringe divergence in Case 3. The longitudinal fringe divergence indicates a fringe divergence of 0.1% at the edge of the measurement volume. By setting the criterion at 0.01%, the useful measurement range along the beam axis is found to be $-0.15\ mm \le z \le 0.15\ mm$. This value is calculated from the following equation.

$$\hat{z}_{\max} = \frac{\sqrt{L_z}}{\left(\cos\left(\arctan\left(\frac{d}{f}\right)\right)\right)^2 \left(\frac{r_o}{d}\right)} \tag{11}$$

Here, $\hat{z}_{\max}$ is the maximum location where the requirement for a given fringe divergence is satisfied. Therefore, a slit or a pinhole, which has an imaged width at the measurement volume less than 0.3 mm is necessary to limit the longitudinal fringe divergence below 0.01%.

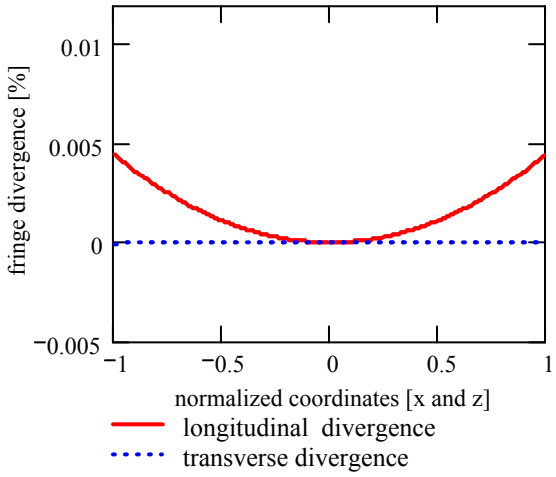

Fig. 2: Fringe divergence for case 1

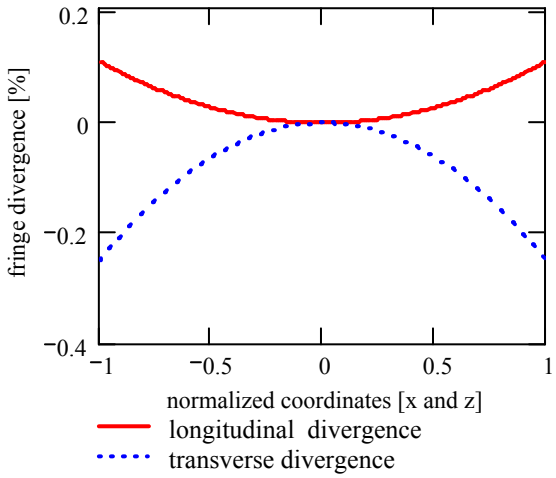

Fig. 3: Fringe divergence for case 2

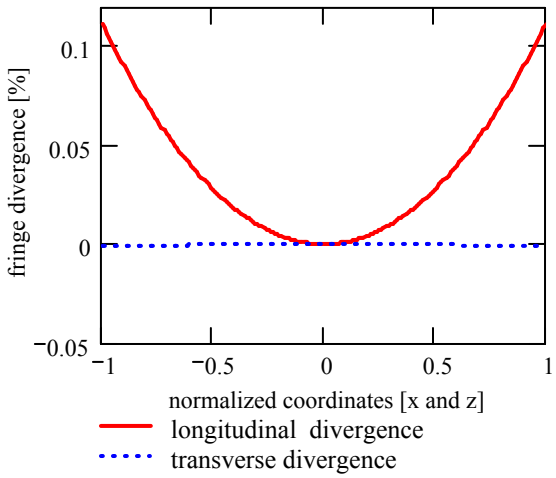

Fig. 4: Fringe divergence for case 3

3. Further Content of Paper

Measurements have been performed in a round free jet and in a stagnation flow. Analytical fluid velocity and acceleration profiles are given by an eddy viscosity approximation. The turbulent structure of a round free jet is also well-documented in the literature, in particular the dependence of dissipation rate, hence the fluid acceleration is known in terms of non-dimensional axial position. Also in the stagnation flow the expected acceleration is known from the mean velocity changes along the stagnation streamline.

Some further remarks will be made about the use of fluid acceleration information in other fields. For instance, in terms of flow noise research, the gradient of fluid acceleration is also important because it gives the dipole component of second-order derivatives of the Lighthill stress tensor T_{ij}. According to the Lighthill's acoustic analogy, the wave equation is derived as follows.

$$\frac{\partial^2 \rho'}{\partial t^2} - c^2 \nabla^2 \rho' = \frac{\partial^2 T_{ij}}{\partial x_i \partial x_j} = \frac{\partial^2 \left(\rho u_i u_j \right)}{\partial x_i \partial x_j} + \frac{\partial a_i}{\partial x_i} - \nabla^2 \left(c^2 \rho'_1 \right) \tag{12}$$

Here, ρ is density, ρ' is density variation, u_i is fluid velocity, a_i is fluid acceleration, c is the speed of sound, ρ'_1 is the density variation in an acoustic source region, and ∇^2 is the Laplacian operator. Even though the last two terms on the right-hand-side are treated as dipole and monopole sound sources on the solid surfaces, they can be also considered as sources by fluid motion. The gradient of Lagrangian fluid acceleration provides one of acoustic sources in this case. Therefore, the gradient of fluid acceleration will be also measured as a first step to evaluate the magnitude of Lighthill stress tensor in the free-air jet and the stagnation flow.

Acknowledgement

This work was supported by the Post-doctoral Fellowship Program of Korea Science & Engineering Foundation (KOSEF).

Literature

Albrecht, H. -E., Borys, M., Damaschke, N., Tropea, C., 2003: "Laser Doppler and Phase Doppler Measurement Techniques," Springer Verlag

Lehmann, B., Nobach, H., Tropea, C., 2002: "Measurement of Acceleration Using the Laser Doppler Technique," Measurement Science Technolology, 13, pp. 1367–1381

Mann, J., Søren, O., Andersen, J. S., 1999. „Experimental Study of Relative, Turbulent Diffusion", Risø-R-1026(EN), Report of Risø National Laboratory, Roskilde, Denmark.

Miles, P. C., Witze, P. O., 1996: "Evaluation of the Gaussian Beam Model for Prediction of LDV Fringe Fields," Proceedings of 9th International Symposium on Application of Laser Technology to Fluid Mechanics, Lisbon, Portugal, pp. 4011–4018

Miles, P. C., 1996: "Geometry of the Fringe Field Formed in the Intersection of Two Gaussian Beams," Applied Optics, 35, pp. 5887–5895